

CHAPTER 2 - STUDY AREA

2.1. GENERAL BACKGROUND OF THE STUDY AREA

2.1.1. Oceanographic studies in North-western Indian Ocean (Arabian Sea)

2.1.2. Historical Background

The origins of “ocean science” in the north-western Indian Ocean, also generally known as the Arabian Sea, extend back to ca. 2,300 B.C., when trade between the Mesopotamian peoples in the Persian Gulf and those of the Indus Valley was established, and trade between Egypt and Somalia (then called Punt) was similarly underway (Warren, 1987). The regularly reversing surface current was not correctly described until A.D. 912, when the traveller El Mas’u’di’ crossed the “sea of the Zanj” as the western Arabian Sea was then known, and described the nature of the Sea, such as the waves, dangers, monsoon winds and currents (Warren, 1987).

Ocean Science came to fruition through the CHALLENGER Expedition of 1873-1876. The expedition greatly expanded man's knowledge of the world's oceans and revolutionized the ideas about planet Earth. However, the Challenger expedition did not survey in the Arabian Sea. The first major oceanographic investigation there, was carried out during 1933-34, on the John Murray MABAHISS Expedition. Exploration increased rapidly in the period 1959-1965, during the course of the International Indian Ocean Expedition (IIOE), with the participation of thirteen nations and at least forty ships. The Geochemical Ocean

Sections Study (GEOSECS) made a survey of the Indian Ocean in 1977-78 covering the Arabian Sea, the Bay of Bengal and the south Indian Antarctic Ocean. The GEOSECS Indian Ocean data are summarized in a compilation of data (Weiss et al. 1983) and in an atlas (Spencer et al. 1982). During the last three decades, comprehensive studies of the physical, chemical and biological oceanography have also emerged as a result of major surveys carried out by Indian Scientists. The investigations have been made during the cruises of the Indian Naval Ships (INS) DARSHAK (1973-74) and R.V. GAVESHANI during 1976 and O.R.V. SAGAR KANYA in the northern Arabian Sea. Recently, other countries have also undertaken expeditions in the Arabian Sea.

Despite this intensive interest, a number of questions remain unanswered. For example, it is not yet clear whether the north-western Indian Ocean (Arabian Sea) is a sink for atmospheric carbon dioxide, due to high rates of primary productivity and burial of sedimentary carbon, or a source via outgassing of carbon dioxide to the atmosphere during upwelling. These processes affect the carbon balance and the global carbon cycle. Furthermore, the Arabian Sea exhibits extremes in atmospheric forcing that lead to the greatest seasonal variability observed in any ocean basin. The wide range of climatic variability in the Arabian Sea, makes it possibly the best place in the present-day ocean to look clearly at past climates and possible future climatic change.

The Arabian Sea has other features which augment monsoonal forcing, thus compelling the basin as attractive site for study. In the north, there is no outlet, but the basin's waters and sediments are influenced by inflow from the Persian Gulf and the Red Sea, and by exchange across the equator. In the following sections, the characteristics of the Arabian Sea are reviewed in detail.

2.2. Setting of the Arabian Sea

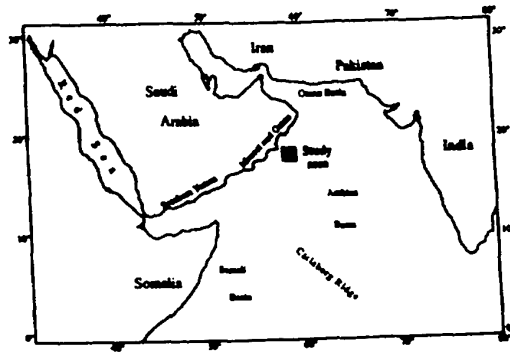
The Indian Ocean is surrounded by an asymmetrical distribution of landmasses characterized by markedly different geology. Although details of their geology are complex, the major shield areas, which surround the ocean basin, namely Africa-Arabia, India, Australia, and Antarctica were formed after the breakup of Gondwana land.

The main physiographic features of the Indian Ocean north of the Equator is shown in Fig.2.1(A, B & C). The Arabian Sea, the area of this study, is bordered by Arabia in the west, Iran and Pakistan to the north and India and the Chagos-Laccadive ridge to the east. The Arabian Sea occupies the total area of about $6.2 \times 10^6 \text{ km}^2$ between 0° and 25° N and 50° and 80° E . The Persian Gulf connects the Arabian Sea through the Gulf of Oman by a 50 m deep sill at the Hormuz Strait. Similarly, the Red Sea is separated from the Arabian Sea through the Gulf of Aden by a 125 m deep sill at the strait of Bab-el-Mandab. The Arabian Sea receives its fluvial input primarily from the Indus River, which drains the Himalayas as well as a large area of semi-arid to arid land in West Pakistan and Northwest India, transporting over 400 million tons of suspended sediments a year. A number of small rivers, chiefly the Narbada, with a common outlet to the Arabian Sea through the Gulf of Cambay, drain the middle portion of India where the soils derive from the weathering of the Deccan Traps. The Narmada and Tapti rivers in India are the only other rivers of significance. The Arabian Basin itself is separated from the Somali Basin by the Carlsberg Ridge, which reduces the flow of bottom water into the Arabian Basin.

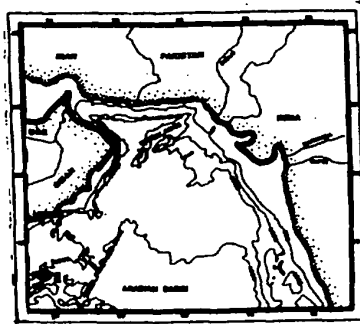
2.2.1. Continental Margin

The continental slope and shelf are wider on the Indian than the Arabian side of the Arabian Sea, therefore exposing a larger area of the sea floor to the oxygen-poor water. Much of the Oman margin is characterized by a narrow continental shelf, bordered by an extremely steep continental formation of the margin (Whitmarsh, 1979; Stein and Cochran, 1985). The continental margin beneath the upwelling zone is a complex mixture of wide and narrow shelves, upper slope basins and ridges, and submarine canyons (Prell et al. 1990; Mountain and Prell, 1989, 1990).

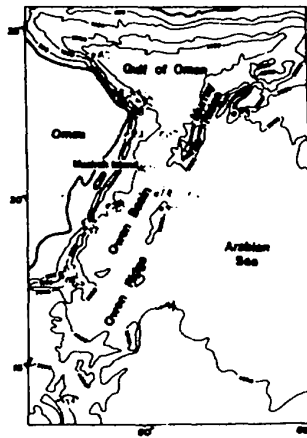
The tectonism of the Oman margin has resulted in the formation of the Owen Ridge and Murray Ridge which separate the Owen Basin from the deep abyssal plain and submarine fan of Indus cone. The Oman basin is roughly triangular in outline and occupies the central floor of the Gulf of Oman at a depth of about 3000 m. The Arabian basin has a maximum depth of 4500 m and merges to the north into the Indus cone.



A



B



C

Figs. 2.1(A, B & C). Map showing main physiographic features of N. Indian Ocean.

The Owen Ridge is an asymmetric, north-east-trending ridge that originates at about 15° 30'N, 59°50'E, where the Sharbithat Ridge intersects the Owen Fracture Zone, and extends to about 20° N, 61°E, where it merges with the Murray Ridge. The trend of the Owen Ridge is somewhat oblique to the Arabian continental margin and its distance from land is about 320 km in the south and about 200 km in the north. The Owen basin, which lies between the Arabian margin and the Owen Ridge, is sediment filled and has depths of 3200-3500 m.

The Owen Ridge lies about 350 to 400 km off the Oman coast and is within their territorial waters. The continental shelf off Oman is characterized by broad wide segments, such as off Sequira, separated by narrow shelves that merge with headland projections, such as off Ras el Madraka. The upper slope of the margin is characterized by several basins that are sub-parallel to the shelf break. These narrow basins lie as shallow as 400 m and as deep as 1,000-1,500 m and result in a step-like margin (Mountain and Prell, 1989, 1990).

2.3. Climatic forcing of the Arabian Sea - the Monsoons

The term 'monsoon' is derived from the Arabic word 'mausim' which refers to the seasonal reversal of winds around the Arabian Sea (Warren, 1966). The Southwest Indian Monsoon system is one of the most important climatic features of the world, impacting most of Africa, southern Asia and the Indonesian archipelago. The success or failure of the monsoon rains in southern Asia and northern Africa affects every phase of life (Prell *et al.* 1992).

The summer season is characterized by high solar radiation that causes intense sensible and latent heating over northern India and the Tibetan Plateau. This pattern of heating causes ascending air flow and the development of an intense low-pressure cell that is centred over Asia at about 30° N (Fig.2.2).

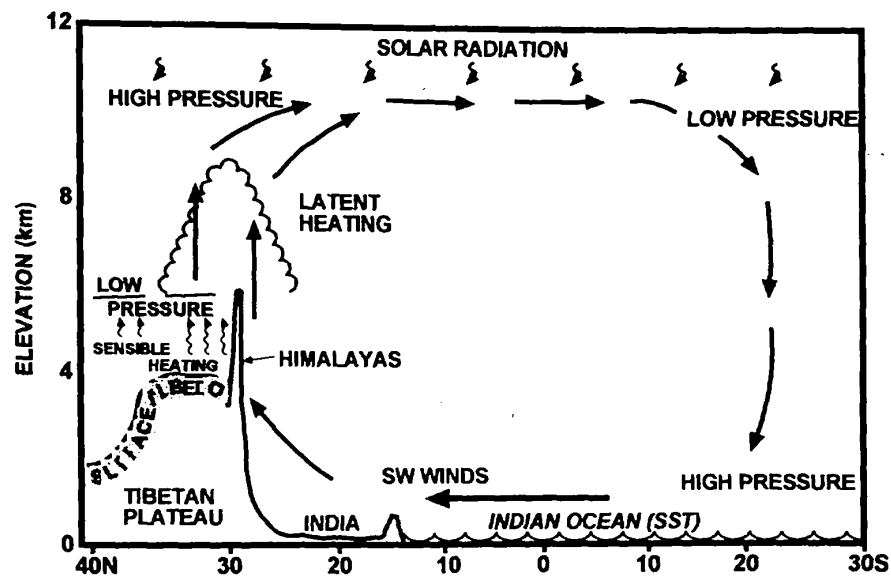


Fig. 2.2. Schematic diagram of the Indian Ocean monsoon geometry and processes (Prell et al. 1992).

2.3.1. Monsoon Systems

Schott et al. (1990) defined the monsoon periods, namely southwest monsoon (June-September inclusive), north-east monsoon (December-February inclusive), autumnal transition (October-November inclusive), and spring transition (March-April inclusive). Only May does not fit into one of the four major monsoonal seasons of the Arabian Sea.

2.4. Physical Oceanography

The climate and hydrography of the Northern Indian Ocean are mainly controlled by the monsoonal circulation. The northern Indian Ocean is different from other major oceans, because of a reversal of the atmospheric and surface oceanic circulations. The major circulation systems in the Indian Ocean can be described (Wyrki, 1973) in three distinct categories namely:

- 1) Seasonally changing monsoonal gyre
- 2) The Southern hemispheric tropical gyre
- 3) The Antarctic waters with circumpolar current

The latter two systems are essentially similar to those of other oceans, whereas the reversing monsoonal gyre is unique to the Indian Ocean. The monsoonal circulation is a direct consequence of the changing wind patterns and the closure of the ocean to the north by the large Asian continent. The monsoon winds are the dominating factor in controlling the surface currents in the Arabian Sea (Fig. 2.3). The currents are stronger during the southwest monsoon; wind changes to the southwest in the summer. The flow in the intermediate layers is not

well known, although it seems that it may also be affected by the monsoonal wind changes (Wyrski, 1971). The winds are predominantly from the north-east during the winter, and the water circulation is cyclonic (counter clockwise).

2.4.1. Water Masses

The deep and bottom water mass circulations, important to near-bottom sedimentary processes and the major transport pathways of the high-salinity water indicating with corresponding depths are shown in Fig. 2.4. Deep water masses are characterized by their density, temperature, salinity and oxygen content. The water masses in the Indian Ocean are:

1. North Indian high-salinity intermediate waters (25-100 m)
2. Antarctic intermediate water (2000-2500 m)
3. Antarctic bottom water/Atlantic deep water (2500-3500 m).

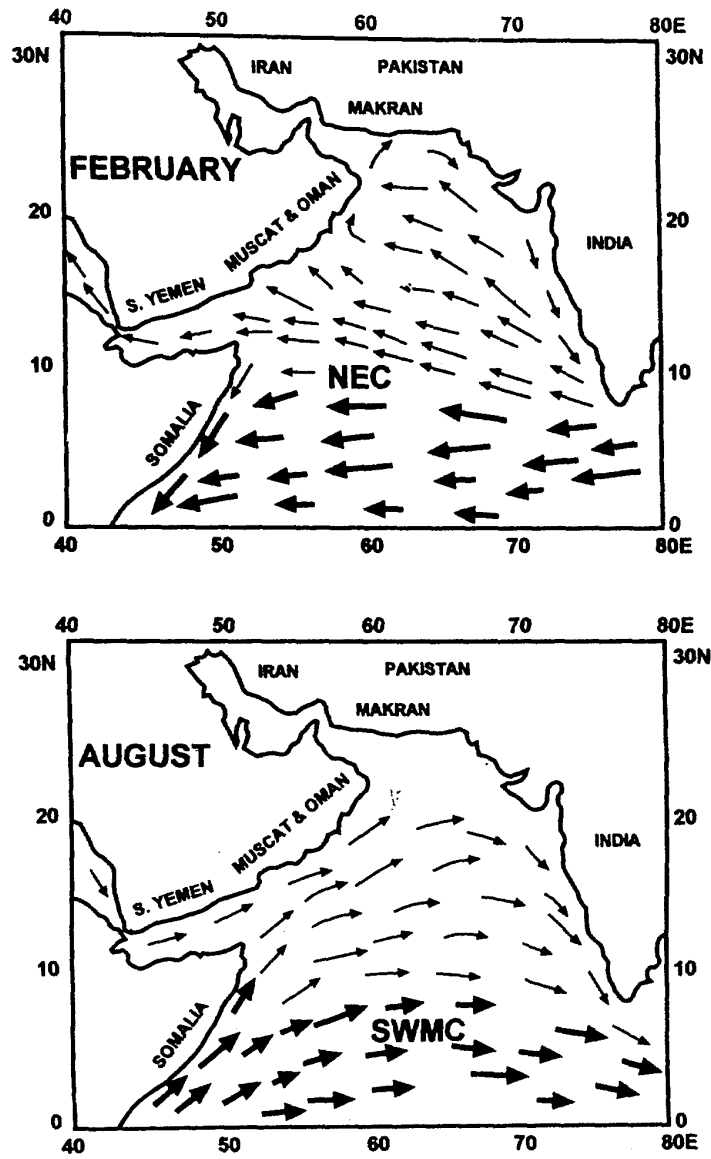


Fig.2.3. Surface currents of North Arabian Sea during NE Monsoon (Nov-Feb) and SW Monsoon (Jun-Aug).

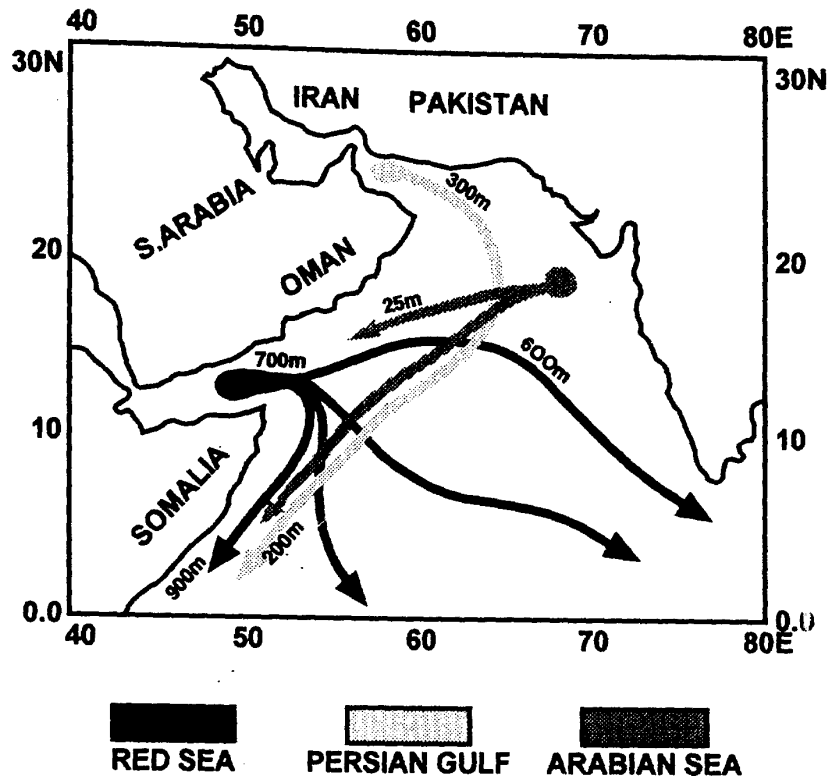


Fig.2.4. The major paths of high salinity water masses of the North Indian Ocean. The numbers shown along the paths represent the depth at that point (Rochford, 1964).

2.4.2. Oman Upwelling System

The monsoonal upwelling system of the Arabian Sea reaches its acme during summer months (Wyrтки, 1971; Krey and Babenerd, 1976; Prell and Streeter, 1982), resulting in high productivity. The strong winds blow from the south-west in summer (rainy season), and from the north-east in the winter (dry season), causing a reversal of the surface circulation from clockwise to anti-clockwise (Wyrтки, 1971). Monsoonal upwelling occurs along the coasts of Arabia and Somalia (Bruce, 1974; Currie *et al.* 1973) and also locally along the west coast of India (Sharma, 1976, 1978). During the southwest monsoonal season, strong offshore Ekman transport of surface waters, leads to their replacement by colder, nutrient-rich waters from several hundred metres deep (Currie *et al.* 1973). The wind speed and the duration of the monsoon control the strength and duration of the upwelling, which in turn causes controls enhanced production of biogenic sedimentary components. By identifying the processes that control the production and preservation of various sedimentary components, the clastic and biogenic components deposited beneath the centres of upwelling can be used to interpret the history of monsoonal upwelling, including upwelling intensity, monsoon strength, and the oceanographic history of surface waters in the northwest Arabian Sea.

2.5. Chemical Oceanography

2.5.1. Salinity

The Arabian Sea has high surface salinity ranges from about 36.2 to above 36.5 due to evaporation. The intermediate waters of the north-west Arabian Sea (200-1000 m of water depth) known as North Indian Intermediate waters (NIIW) are characterized by high salinity (34.8; Wyrтки, 1971, 1973) and by spatial and temporal stability. The Red Sea and the Persian Gulf overflows, which spread at about 800 m and 300 m, respectively, are the sources for the intermediate waters (Swallow, 1984).

2.5.2. Nutrients

During SW Monsoon periods, the nutrient concentrations are higher in surface coastal waters off both Somalia and Arabia (Wyrтки, 1971; Qasim, 1982). In the offshore regions the concentrations are lower indicating more consumption with higher productivity during the SW Monsoon periods (Reddy and Sankaranarayanan, 1968). The levels of nutrient are inversely correlated to dissolved oxygen due to organic matter degradation (Ryther *et al.* 1966).

2.6. Primary Production

The Arabian Sea is an area of high productivity averaging about twice that of the world oceans (Ryther et al. 1966), and productivity is unique in its magnitude among all oceans of the Northern hemisphere at these latitudes (Yoder et al. 1991). High productivities are especially apparent in the north-western sector (Qasim, 1977; Sen Gupta and Naqvi, 1984) due to the very high nutrient concentrations. In response to richer nutrient supplies, the annual rates of primary production in the northern Arabian Sea averages $>500 \text{ mg C/m}^2/\text{day}$ in May to October, dropping to values as low as $150 \text{ mg C/m}^2/\text{day}$ during November to April (Krey and Babenerd, 1976, Qasim, 1982). Daily rates can exceed $2 \text{ g C m}^{-2} \text{ d}^{-1}$ (Qasim, 1982), reaching perhaps $6 \text{ g C m}^{-2} \text{ d}^{-1}$ (Babenerd and Krey, 1974). The unusual atmospheric forcing of the region also creates areas of high primary productivity that are adjacent to areas of perennially low primary production.

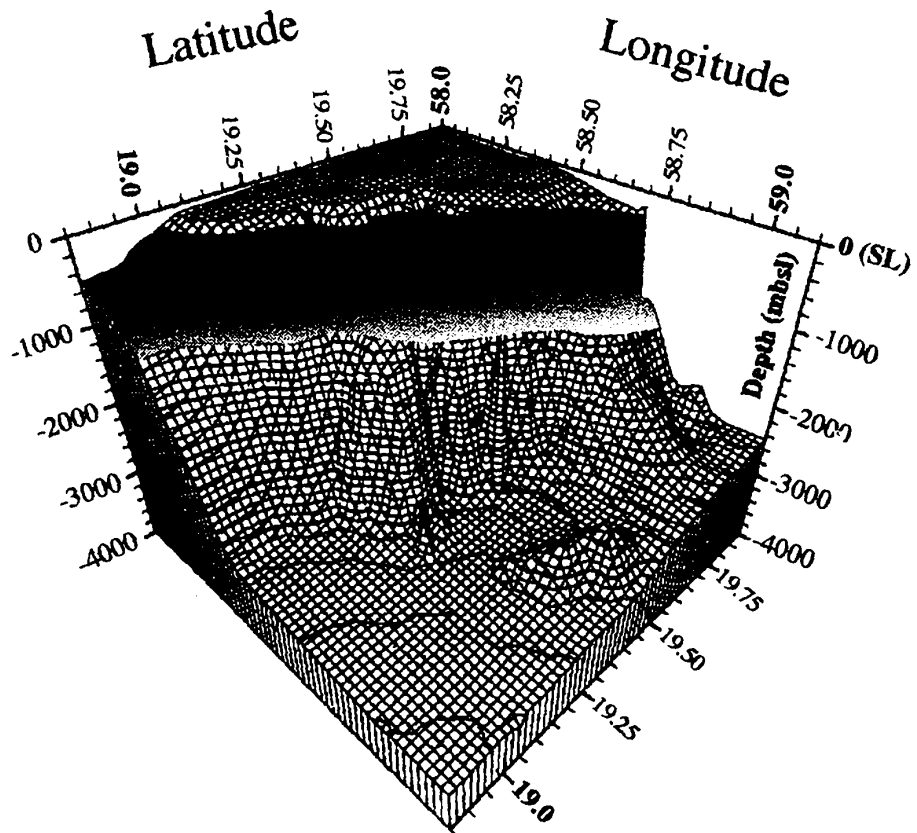
2.6.1. Plankton Patterns

The sediments are characterized by a variety of fossil plankton (both phytoplankton and zooplankton) that are associated with active upwelling and its productivity (Prell, 1984; Cullen and Prell, 1984; Kroon, 1988). For example the foraminiferan species, Globigerina bulloides, seems to be associated with tropical upwelling systems. Outside sub-polar waters, G. bulloides is abundant only in the western Arabian Sea and the Cariaco Basin in the Caribbean, which is also a seasonal upwelling system (Peterson et al. 1991). G. bulloides exhibits distinct abundance gradients and constitutes more than 40% of all of the planktonic

foraminifera preserved in the sediments along the coast of Oman and decreases seaward (Prell *et al.* 1992). The distribution of *G. bulloides* in the sediments and its relation to seasonal temperature and chemical indices of upwelling, indicates that its abundance is linked to the highly productive periods of the southwest monsoon. High rates of foraminiferan flux during the south-west monsoon season are predicted from the sediment record and sediment trap data.

2.7. Oxygen Minimum Zone

An important characteristic of upwelling areas is the oxygen minimum zone (OMZ) that lies below the source waters of the upwelling system (Margalef and Estrada, 1981). A water mass representing an oxygen minimum layer is present (Fig.2.4A) between ~ 200-1200 m.b.s in the northern Indian Ocean, including the Arabian Sea and Bay of Bengal. The stable zone of oxygen depletion, the OMZ, is produced by the combined effect of restricted horizontal advection of central Indian Ocean water, such as the Persian Gulf, Red Sea, and Banda Sea waters, which are relatively impoverished in oxygen, stable salinity and temperature stratification, and high chemical oxygen demand due to upwelling-related high productivity ($>500 \text{ mg C/m}^2/\text{day}$). These lead to the development of the OMZ, with extremely low oxygen concentrations of less than 0.5 mL/L (Wyrтки, 1971, 1973; Slater and Kroopnick, 1984). The oxygen-deficient layer is intercalated between the oxygen-rich and highly productive shallow mixed layer and the deeper layers originating from circumpolar and North Atlantic deep waters. The northern part of the Owen Basin shows the most



Oxygen Minimum Zone

Fig. 2.4 A. Map showing Oxygen Minimum Zone in the Arabian Sea.

severe depletion of oxygen (Price and Shimmield, 1987; Hermelin and Shimmield, 1990).

The sub-oxic portion of the OMZ in the Arabian sea is located in the eastern portion of the basin and is one of the three most sub-oxic regions of the global oceanic water column. The other two are found in the eastern tropical north and south Pacific Ocean (e.g. Codispoti and Richards, 1976; Codispoti and Packard, 1980). The oxygen deficient zone is a site of intense denitrification, contributing perhaps as much gaseous nitrogen to the atmosphere as the eastern tropical Pacific Ocean.

2.8. Particle flux

The monsoonal upwelling season increases the flux of material to the sea floor, as observed from preliminary data of sediment trap studies by Indo-German, and US programmes. Nair et al. (1989) used time-series sediment trap experiments to show that the particle flux to the seafloor in the western Arabian Sea is strongly seasonal, with a primary peak during the summer southwest monsoon and a secondary peak in winter. The sediment trap data revealed that the modern lithogenous fraction (80%) is transported to the western Arabian Sea during the summer monsoon (Nair et al. 1989). The sediment trap data obtained at about 60° E during the monsoon seasons of 1986 and 1987 and the intervening winter (Curry et al. 1992) revealed a flux of 15,000 planktonic foraminifera m⁻² d⁻¹. During the non-monsoonal period, the flux was less than 1000 planktonic foraminifera m⁻² d⁻¹. The westernmost part of the basin shows higher biogenic

fluxes compared to the central and eastern Arabian Sea (Curry et al. 1992; Nair et al. 1989). The results of the sediment trap data further suggest that carbonate is dominant rather than opal in the western Arabian Sea upwelling system and coccolithophores are unusually abundant (Nair et al. 1989; Murray and Prell, 1992).

The strong seasonal cycle in carbon fixation and transformation, alternating between highly eutrophic and fairly oligotrophic conditions is evident in material captured in sediment traps. The south-west and north-east monsoon periods showed greater variability than eastern and western sides of the basin within either monsoon period (Nair et al. 1989). Empirical relationships developed for the world ocean (Suess, 1980; Betzer et al. 1984) suggest that the higher primary production of the nearshore region off Oman is carried offshore and eastward by the vigorous surface currents of the south-west monsoon and is deposited at depth downstream at a fairly rapid rate. The observed deposition and that predicted from primary production in the north-east monsoon period are reasonably similar at all three of Nair's et al.'s (1989) trap locations (western, central and eastern Arabian Sea). The transition periods showed greater fluxes to sediment traps following the south-west monsoon than it in periods leading up to the south-west monsoon.

2.9. Sediments/Sedimentology

The continents surrounding the Indian Ocean have vast areas of inland desert, bordered on the west and north by the major arid lands such as the Thar desert of India, Rubulkhali in SW Arabia, coastal Makran of Iran and Pakistan and lowlands of Mesopotamia and Africa (Fig. 2.5) and it is known that a substantial fraction of the bottom sediments of the NW Arabian Sea are derived from aeolian sources (Thiede, 1974; Whitmarsh *et al.* 1974; Weser, 1974; Sirocko *et al.* 1991).

The main trajectories of aeolian transport (Fig. 2.5) into the NW Arabian Sea originate from the surrounding deserts (Coude-Gaussen, 1984). The other major supply of lithogenic allochthonous materials derive from the rivers Indus (Ittekkot and Arain, 1986), Narmada and Tapti (Borole *et al.* 1982) mainly during the SW Monsoon. There are no riverine inputs from the Arabian Peninsula or northern Africa (Kolla *et al.* 1981). The estimated annual aeolian dust input to the Arabian Sea is equivalent to the riverine inputs (Sirocko and Sarnthein, 1989).

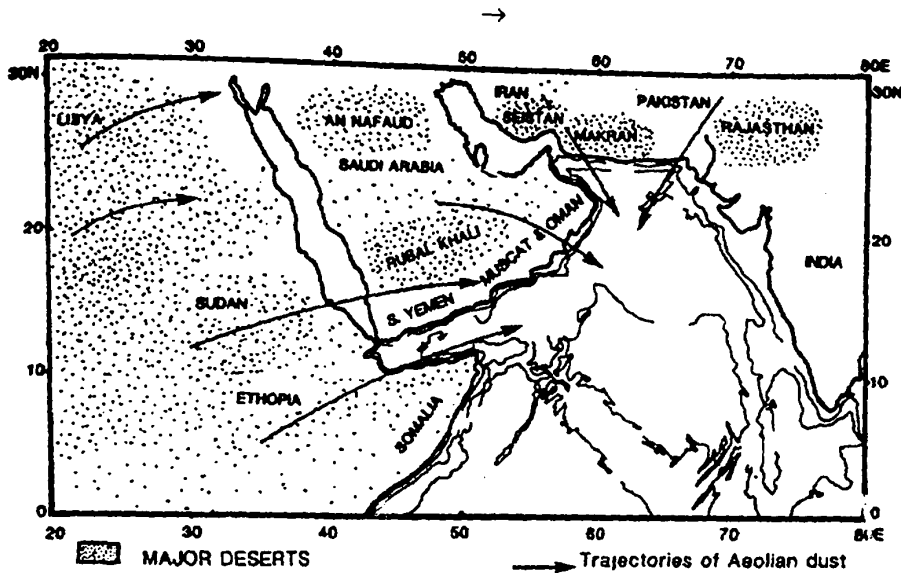


Fig. 2.5. The major bordering deserts areas in the Arabian Sea.

Arrows represent the main trajectories of aeolian dust after Coude-Gaussen, 1984.

2.9.1. Distribution of Sediments

The sediments of the northern Indian Ocean record a wide variety of paleoceanographic and paleoclimatologic responses, many of which are related to the southwest monsoon circulation. The marginal areas of the northern and western Arabian Sea exhibit coarse grained sediments that are low in carbonate content with large amounts of quartz and feldspar indicating significant terrigenous sedimentation (Kolla *et al.* 1981). However, the continental slope is

very high in carbonate, indicating mostly marine sedimentation. Kolla *et al.* (1981) reported a sedimentation rate of 4 cm ky^{-1} in water depths of 2000-3500 m of the Arabian peninsula. Most of the sediments on the margin are bioturbated, even though oxygen values in the bottom water on the margin are as low as 0.2 mL/L. In general, margin sediments bear a continuous imprint of constant high surface productivity, while facies changes signify changes in the depositional environment. Sediments of the western Indian Ocean are often significantly affected by the continental climate and geology or southern ocean volcanism, and by long-distance sediment transport through oceanic surface circulation, Antarctic Bottom Water movements, turbidity currents, or aeolian processes (Kolla *et al.* 1976).

2.9.2. Sediments in the Upwelling Zone

The Arabian Sea sediments are strongly influenced by the upwelling at its western and eastern margins (Smith, 1968). The marginal basin sediments are extremely organic-rich, accumulating at rates of 10 to 20 cm ky^{-1} (Prell, Niituma, *et al.* 1989). The sediments have a surprisingly high ratio of carbonate when compared to those of other upwelling zones. These sediments accumulate rapidly within the OMZ (*i.e.* ~200 m to 1500 m, see above 2.7). There seems to be a relationship between productivity in upwelling zones, organic carbon content and the history of the OMZ at the site. If low oxygen concentration were low enough to prevent bioturbation, one would expect to find annually laminated sediments preserved annually in the Oman Margin. Laminated sediments are observed off Bombay and in the Gulf of Aden, but presently not off Oman.

However, laminated sediments of age about 1 to 3.4 Ma, were obtained during ODP drilling off Oman, indicating that low oxygen contents led to the preservation of annual laminations at this time (Prell, Niitsuma, et al. 1989).

Deep-Sea Drilling project studies on deep-sea sediments have also revealed the effect of fluctuation in monsoon strength on the changes in productivity cycles. During the last glacial maximum (18 kyr B.P) monsoon winds were weaker, there was a lower upwelling intensity and the Arabian sea was warmer than today (Prell et al. 1990).

2.10. Organic/Inorganic Geochemistry of the Arabian sea

Although, the Arabian Sea sediments are enriched in organic and inorganic carbon, the biological and chemical processes leading to their distribution are not well defined. The organic carbon contents of sediments are greater than 2% and reach up to 8% in some basins, reflecting high organic fluxes (Prell et al. 1992). Some sediments are rich in organic carbon, even when remote from the sources of high productivity.

Various hypotheses have been proposed regarding the control of the distribution of organic carbon in the Arabian Sea sediments: i) primary productivity, ii) rate of sedimentation, iii) the concentration of dissolved oxygen in the water overlying the sediments, iv) enhanced terrigenous sedimentation; v) bottom water anoxia together with sedimentological parameters such as the texture of the sediments.

The continental slope off western India shows maximum sedimentary organic carbon content at water depths where the oxygen minimum intersects the

seafloor (Schott et al. 1970; Marchig, 1972; von Stackelberg, 1972). This has led to the suggestion that the bottom water oxygen concentration on this margin controls the abundance of organic carbon in the surface sediments (Schlanger and Jenkyns, 1976; Thiede and Van Andel, 1977; Slater and Kroopnick, 1984; Paropkari et al. 1992, 1993).

In contrast, the organic carbon maximum on the continental slope of the eastern Arabian Sea has no relation with the oxygen minimum. This suggests that the OM distribution on the western Indian Continental margin is controlled by the depth-related settling fluxes of organic carbon to the sea floor (decreasing westward away from the centres of coastal upwelling and also decreasing with increasing water depth), dilution by other sedimentary components, textural control of the sediments (coarser-grained sediments having lower carbon contents) together with the combination of sediment supply and reworking (Calvert et al. 1995; Paropkari et al. 1992).

CHAPTER 3 - MATERIALS AND METHODS

3.1. TRACE METAL ANALYSIS

3.1.1. Chemical Leaching Technique for the determination of trace metals in sediments

There are number of workers who have attempted to classify sediments on the basis of generic components. Kryine (1948) used a simple two fold scheme to separate detrital (transported in a solid form) and non-detrital (transported in a dissolved form) fractions. Goldberg (1954) described a detailed classification of the components into lithogenous, biogenous, hydrogenous, cosmogenous and interstitial water categories. These schemes are useful to the geochemist for the analytical separation of different classes of components (Table 3.1).

Table 3.1. The major trace element binding phases in sediments (after Förstner and Patchineelam, 1976).

Binding Phase	General Type of Bonding Mechanism
Silicate minerals Heavy minerals	Incorporated into mineral lattice structures; <u>e.g.</u> element-oxygen bonds.
Hydrous oxides of iron and manganese	1. physical adsorption 2. chemisorption 3. coprecipitation
Calcium carbonate	1. physical adsorption 2. pseudomorphism 3. coprecipitation
Organic matter; <u>e.g.</u> humic, lipid and bituminous	1. physical adsorption 2. chemisorption 3. complexation/precipitation
Heavy metal precipitates; <u>e.g.</u> carbonates, phosphates hydroxides and sulphides	Transgression of the solubility product of the relevant heavy metal salt

The chemical leaching technique is a method for the accurate determination of various phases of element associations in sediments (exchangeable, carbonates, oxides and sulphides etc.) in terms of their environmental significance (Table 3.2). Thus, it can provide information on the mobility and availability of elements in the sediments, and therefore on the effect that diagenetic reactions will have on the geochemistry of trace metals in oceanic sediments.

Table 3.2. Operationally defined trace metal binding phases in sediments (e.g. Tessier et al. 1979).

Sequential leaching stage	Binding Phase	Notes (Chester <u>et al.</u> 1988)
1	Exchangeable fraction	-----
2	Carbonate or surface associated	Associated with phases such as hydrous iron and manganese oxides, clays, etc.
3	Easily reducible fraction	e.g. 'New' oxides and oxyhydroxides of manganese and amorphous iron oxides
4	Moderately reducible fraction	e.g. 'Aged' manganese oxides and crystalline iron oxides
5	Organically or sulphide bound	If present, may be sulphide bound
6	Residual fraction	Mainly lattice-held positions in lithogenous minerals

The reagents used in chemical leaching are selected in such a way as to dissolve discrete fractions of a sediments (see e.g: Goldberg, 1954; Agemain and Chao, 1976; Förstner and Patchineelam, 1976; Tessier et al. 1979; Chester and Voutsinou, 1981; Chester et al. 1985; Towner, 1984; Kersten and Förstner, 1987). They need not be species selective but are 'operationally-defined'. Sequential leaching

studies can distinguish between the distribution of metals in the detrital (or refractory) and non-detrital (or non-refractory) fractions of sediments (see e.g.: Chester and Messiha-Hanna, 1970, Chester and Voutsinou, 1981). Trace metals associated with the detrital fractions are held in the internal matrix structure of aluminosilicate and other detrital minerals, whilst the non-detrital fractions of metals are fixed in a number of non-matrix associations, some of which are more stronger than others. A two stage leaching technique that distinguishes between detrital and non-detrital metals can be applied as a rapid and simple method to obtain information on the storage of elements and the detection of the degree of metal pollution in sediments, but it will mask any subtle geochemical associations in the non-detrital fraction itself. Multi-stage sequential leaching techniques are therefore often employed, and have been extensively reviewed by Towner (1984) and Thomas (1987). The scheme applied in this study (Table 3.3) is the ‘best working compromise’, linking operationally-defined host separations with geochemically meaningful fractions. The scheme was initially proposed by Tessier et al. (1979) and modified later by Towner (1984) and Thomas (1987) (see Table 3.2). The modifications of the schemes were as follows:

- 1) The magnesium chloride reagent (stage 1) was replaced by ammonium acetate, because the former attacks carbonates (Tessier et al. 1979; Towner, 1984). The use of ammonium acetate also alleviates the more serious matrix problems encountered with magnesium chloride in GF-AAS; e.g. interference in lead determinations as a result of the formation of lead chlorides in the graphite furnace (Sturgen and Chakrabarti, 1978).

- 2) An additional step (stage 3) was incorporated into the scheme to differentiate between the easily reducible fraction (mainly manganese oxy-hydroxides with small amounts of amorphous iron oxides) and the moderately reducible fractions (mainly

crystalline iron oxides, together with some resistant manganese oxides). The reagent used for this purpose was sodium acetate (1 M) plus hydroxylamine hydrochloride (0.25 M).

Table 3.3. Sequential leaching schemes used by Tessier et al. (1979), Towner (1984) and Thomas (1987).

Phase	Sequential leaching scheme			Sequential leaching stage
	1	2	3	
Exchangeable fraction	MgCl ₂	MgCl ₂	NH ₄ OAc*	1
Carbonate fraction	NaOAc	NaOAc	NaOAc	2
Easily-reducible fraction	_____ ↑	NaOAc / NH ₂ OH.HCl	NaOAc / NH ₂ OH.HCl	3
Moderately-reducible	HOAc / NH ₂ OH.HCl	HOAc / NH ₂ OH.HCl	HOAc / NH ₂ OH.HCl	4
Organically bound fraction	H ₂ O ₂ / NH ₄ OAc	H ₂ O ₂ / NH ₄ OAc	H ₂ O ₂ / NH ₄ OAc	5
Residual fraction**	HF/HClO ₄	HF/HNO ₃	HF/HNO ₃	6

1. Tessier et al. (1979)

2. Towner (1983)

3. Present Study

* modification by Thomas (1987)

** stage 6 was not analysed in this study.

3.1.2. Cleaning Procedure

All glassware and polypropylene boiling tubes were cleaned by soaking in an acid bath (10% HNO₃, 24 h), rinsed with Milli-Q water (18.2 M Ω cm⁻¹) and dried in an oven (~60°C). Volumetric flasks and graduated measuring cylinders were treated in the same way but dried at room temperature.

3.1.3. Chemicals

The following chemicals were used for sequential leaching:

- 1) Milli-Q water (18 MΩ cm⁻¹ resistivity) was used for the reagents and standard preparations.
- 2) Nitric acid (16 M ; AnalaR grade), BDH. This reagent was purified by redistillation of ‘AnalaR’ grade acid in a distillation apparatus fitted with a quartz stillhead and condenser. The redistilled concentrated acid was then diluted to 0.1 M with Milli-Q water and was used for making up extractants and standards.
- 3) Ammonium acetate (1 M ; AnalaR grade, BDH).
- 4) Sodium acetate (1 M ; AnalaR grade, BDH).
- 5) Hydroxylamine hydrochloride (25 % ; AnalaR grade, BDH).
- 6) Hydrogen Peroxide (30% ; AnalaR grade, BDH).
- 7) Acetic acid (Redistilled; AnalaR grade, BDH). This reagent was purified by redistillation of ‘AnalaR’ BDH grade acid (as above).

3.1.4. Apparatus

- 1) Volumetric flasks (25 mL) were used for making up the standard and extractants to known volumes.
- 2) Polypropylene boiling tubes (50 mL) were used for the extraction procedure.
- 3) Pre-cleaned polyethylene containers were used for storage of reagents.
- 4) Linear polystyrene ('Sterilin') bottles (30 mL) were used for storage of samples and standards prior to analysis.
- 5) A Janke & Kunkel (IKA[®] - Labortechnik KS 501D) mechanical orbital shaker was used to agitate samples to ensure uniform reaction of sample and reagent .
- 6) A MSE 'Centaur 1' centrifuge was used (3000 r.p.m) for the separation of the residue from the solution where necessary.
- 7) A sand bath was used to heat samples for Stages 4 and 5 at the required temperature.

3.1.5. Reagent Preparation

(Stage 1) Surface adsorbed, or exchangeable, ions

Preparation of ammonium acetate solution (1 M)

Ammonium acetate (77 g) was dissolved in water (Milli-Q, 1000 mL) and the reagents were passed through a 10 cm ion exchange column containing 'Chelex 100' resin in the ammonium form, to remove any trace metals present. The pH of the solution was then adjusted to 7.0 with redistilled acetic acid.

(Stage 2) Carbonate-associated and chemisorbed ions

Preparation of sodium acetate solution (1 M)

Sodium acetate (136.08g) was dissolved in water (Milli-Q, 1000 mL) and cleaned as for stage 1. The pH of the reagent was then adjusted to 5.0 with redistilled acetic acid.

(Stage 3) Easily reducible (manganese) oxides

Preparation of hydroxylamine hydrochloride (0.25 M)/Sodium acetate solution

(1 M)

Hydroxylamine hydrochloride (17.4 g) was added to sodium acetate (1 M) dissolved in water (Milli-Q, 1000 mL). The pH was adjusted to 5.0 with redistilled acetic acid.

(Stage 4) Moderately reducible (iron) oxides

Preparation of hydroxylamine hydrochloride solution (0.25 M) plus acetic acid (25 % v/v)

Hydroxylamine hydrochloride (17.4 g) was dissolved in water (Milli-Q, 250 mL) and redistilled acetic acid (250 mL) and made up to 1000 mL.

(Stage 5) Peroxidisable organic fraction

Preparation of ammonium acetate solution (1 M)

Ammonium acetate (77 g) was dissolved in water (Milli-Q, 1000 mL) and the pH adjusted to 2.0 with nitric acid. This reagent was added together with hydrogen peroxide (30%) and redistilled nitric acid (0.01 M) as detailed in Table 3.4.

Table 3.4. Sequential Extraction Procedure

Fractions	Reagents	Experimental conditions		
		Vol. (mL)	Time (h)	Temp.(°C)
Surface adsorbed/ exchangeable	1M NH ₄ OAc (pH 7)	10	0.25	25
Carbonate	1M NaOAc (pH 5)	20	5	25
Easily-reducible	1M NaOAc + 0.25M NH ₂ OH.HCl (pH 5)	20	16	25
Moderately-reducible	0.25M NH ₂ OH.HCl	20	6	90
Organic	30% H ₂ O ₂ + 0.01M HNO ₃ +1M NH ₄ OAc	see note below		

3.1.6. Sequential Leaching Extraction Procedure

A dried sediment sample was homogenised using a pestle and mortar, then the sample (~50-200 mg) was accurately weighed into a polypropylene boiling tube. The first reagent (stage 1, 10 mL) was added to the sample and the tube covered with a piece of clingfilm in order to avoid contamination from the cap. Care was taken to allow minimal contact between the reagent and the clingfilm and the tube was shaken on a mechanical shaker (15min; 25°C). The polypropylene tube was then centrifuged (15 min; 3000 r.p.m). The supernatant liquid was decanted into a volumetric flask and made up to volume with redistilled HNO₃ (0.1 M; stage1, 10 mL and stage 2-5, 25 mL). The respective leaching solutions were transferred after each stage into Sterilins tubes (30 mL) for storage prior to analysis.

The remaining solid residue after each stage was treated, respectively, with the next stage reagent. A similar method of shaking and centrifuging was followed as mentioned below (see Table 3.4).

Stage 2 reagent (20 mL) was added to the stage 1 residue in the boiling tube, and the tube was shaken on a mechanical shaker (5 h ; 25° C) and then centrifuged (15 min.).

Stage 3 reagent (20 mL) was added to the stage 2 residue in the boiling tube, and the tube was shaken on a mechanical shaker (16 h; 25° C) and then centrifuged (15 min.).

Stage 4 reagent (20 mL) was added to the stage 3 residue in the boiling tube, and heated in a sand bath (90° C ; 6 h).

For Stage 5, H₂O₂ (5 mL) and HNO₃ (0.01 M; 3 mL) were added to the residue in the boiling tube and heated (85°C ; 2 h), after which further portions of H₂O₂ (3 mL)

and HNO_3 (0.01 M; 2 mL) were added and samples heated (85°C ; 3 h). The solutions were allowed to cool prior to addition of NH_4OAc (1 M; 10 mL). The tubes were shaken continually (16 h) and centrifuged.

Extractions were performed along with in-house standard reference materials and analyses was carried out within two days of the extraction of leached elements.

3.1.7. Preparation of Standard Solutions

Mixed (multi-element) standards were made up from BDH ‘Spectrosol’ stock solutions (1000 ppm) in a redistilled nitric acid (0.1 M) matrix and stored in ‘Sterilin’ containers until required. An initial mixed standard (100 ppm) was made up and then aliquots were diluted with respective sequential leaching solutions to give a range of standards (10, 20, 50 ppb, 0.1, 0.2, 0.5, 1.0 and 2.0 ppm) in Sterilin bottles. Because of the large number of sample analyses involved, it was not possible to adopt a standard additions method to eliminate matrix effects. Instead, sample and standard matrices were closely matched (*e.g.* Lachica and Barahona, 1993). For this purpose, a range of standard solutions was prepared using the following matrices which correspond to the individual sequential extraction stages.

(Stage 1) Ammonium acetate solution (1 M).

(Stage 2) Sodium acetate solution (1 M).

(Stage 3) Hydroxylamine hydrochloride (0.25 M)/Sodium acetate solution (1 M).

(Stage 4) Hydroxylamine hydrochloride solution (0.25 M) plus acetic acid (25 % v/v).

(Stage 5) Ammonium acetate solution (1 M)+Hydrogen peroxide (30%) and redistilled nitric acid (0.01 M).

The standards were all handled in a dust-free room with critical stages of preparation being performed in a clean air cabinet. Autopipettes were used to transfer quantities of the standards, with appropriate changes of pipette tips to avoid contamination.

3.1.8. Instrumentation

3.1.8.1. Flame AAS

All determinations of Mn and Fe were made on a Perkin-Elmer model 2380 flame atomic absorption spectrophotometer. The analytical conditions are shown in Table 3.5. All the flame measurements were made on a double beam dual channel (*i.e.* both the hollow cathode lamp (or EDL) and the BG deuterium arc lamp are present) using single element hollow cathode lamps. This has the capability of simultaneous background correction using a deuterium lamp. For the determination of Mn, Fe and Cu (if above detection limits) concentration, an air-acetylene flame was used.

Table 3.5. Instrumental Conditions for the Perkin-Elmer 2380 AAS.*

Flame AAS

Element	Wavelength (nm)	Slit width (nm)	Flame	Sensitivity (ppm)	Linear range (ppm)
Manganese	279.5	0.2	Air-acetylene	0.052 (FS) 0.030 (IB)	2.0 (FS) 2.0 (IB)
Iron	248.3	0.2	Air-acetylene	0.100 (FS) 0.039 (IB)	5.0 (FS) 2.0 (IB)
Copper	324.8	0.7	Air-acetylene	0.077 (FS) 0.032 (IB)	5.0 (FS) 2.0 (IB)

Note FS - Flow Spoiler ; IB - Impact Bead

* as recommended in the manufacturer manual (Perkin-Elmer).

Both the standard and sample solutions were aspirated directly into the flame, but dilutions were made whenever the sample concentrations were beyond the upper limit of the linear range.

Calibration curves were constructed from known standards (in an appropriate matrix) to obtain the linear working range for individual elements in each matrix. The calibration curves were re-determined periodically (*ca.* every 6 samples) to check for drift in the baseline during a series of determinations. Blanks were run together with each batch of samples to take into account reagent, or other, sources of contamination. Where blank readings were significant, these were subtracted from the concentrations obtained for the sample.

3.1.8.2. Graphite AAS

Copper was generally present in low concentrations which required the use of graphite furnace AAS. A Perkin-Elmer AAS (Model 1100 B) equipped with deuterium background correction, an AS-70 auto sampler, HGA 700 furnace programmer and EPSON.FX-850 Printer Sequencer was used. Single element hollow cathode lamps were employed and argon was used as the carrier gas. The appropriate wavelengths, lamp currents and other conditions for the determination of Cu were selected from the Perkin-Elmer reference manual as a guide in developing the program conditions. However, the optimum temperature and time required for a particular stage in a

particular matrix, was used to obtain the maximum sensitivity and/or greatest working (linear) range for Cu (see Appendix A).

Calibration curves were constructed from known standards (in the appropriate matrix) to obtain the working range for Cu in each matrix. In graphite furnace AAS, matrix matching of samples and standards is very important, since the technique suffers from matrix effects, even though in theory, the matrix is removed before the sample is atomised. Apart from this, ‘memory effects’ found between individual determinations, may arise during the use of graphite furnace due to metal impactions onto graphite tube walls. The use of pyro-coated graphite tubes and appropriate programmes reduces this problem. The pyro-coated tubes have also been found to be more resistant to corrosive matrices and severe temperature programs selected (e.g.) to volatilise Na^+ in stages 2 and 3), and to have longer life spans.

Reagent blanks were run concurrently with samples to check for any possible reagent, or other operationally associated, contamination. Necessary corrections were made in the determination of sample concentration, where significant blank values were observed.

3.1.9. Determination of Trace Metals

The following equation was used to calculate the concentration of each element in the sediment sample.

$$C_E = (A \times B) / SW \text{ } \mu\text{g/g}$$

C_E = Concentration of element ($\mu\text{g/g}$)

A = Concentration of element in solution ($\mu\text{g/mL}$)

B = Volume of extracted solution (mL)

SW = Sediment weight (g)

3.1.10. Reproducibility

Analytical reproducibility was determined by duplicate analyses of extracts of in-house standard reference materials which were analysed routinely with each batch of samples. A Mersey sediment used for this purpose was originally prepared by mixing and homogenising several sediment samples collected from the River Mersey. The analytical development and reproducibility experiments have been carried out previously in these laboratories by a number of workers.

The analytical precision of the sequential leaching scheme (Table 3.3) was determined by sequential analysis of a Mersey sediment (in duplicate) and the results are reported below (see Table 3.6).

Table 3.6. Concentrations of trace metals in each operationally-defined non-detrital fractions of Mersey sediment.

Element	Concentration ($\mu\text{g/g}$)					Σ Conc. ($\mu\text{g/g}$)	
	Stage 1	Stage 2	Stage 3	Stage 4	Stage 5		Stage1-5
Iron	(1)	N.D	464.2	849.6	2943.5	1052.6	5309.9
	(2)	N.D	463.5	758.2	2533.0	1051.0	4805.7
Manganese	(1)	40.7	371.7	79.6	84.0	26.4	602.4
	(2)	50.5	408.9	88.8	85.5	29.0	662.7
Copper	(1)	5.0	13.3	0.5	12.3	16.6	47.7
	(2)	6.0	10.3	0.5	9.4	16.7	42.9

(1) and (2) are duplicates.

3.2. Carbohydrates Analysis - Total hydrolysable carbohydrates (THCH)

3.2.1. Introduction

The group of carbohydrates or carbohydrate-like compounds determined in this study includes not only the simple sugars, but also oligo-and polysaccharides which are broken down to monosaccharides by acid hydrolysis. The estimation of total carbohydrates is sufficient when mass balance of organic matter, or correlation with total organic matter is required and direct analysis with a non-specific colorimetric test, using a glucose standard can be applied (Rogers, 1965; Swain, 1966, 1967 and Gerchakov and Hatcher, 1972).

The phenol-sulphuric acid method was described originally as a non-specific quantitative test for carbohydrates (Dubois *et al.* 1956). The colorimetric test is based on

the formation of an orange complex on reaction of phenol, sulphuric acid and a carbohydrate. It is often preferred for total carbohydrate analysis, because its molar absorptivities for most sugars fall within a narrow range; unlike those observed for various sugars by other methods. The phenol-sulphuric acid method has been used for the determination of total carbohydrates in sediments (Artem'yev, 1969, 1970) and in particulate matter (Handa, 1967) after hydrolysis (Dubois et al. 1956; modified by Gerchakov and Hatcher, 1972), with spectrophotometric monitoring at a wavelength of 485 nm (see Fig. 3.1). Handa (1966) suggested the phenol method for the determination of carbohydrates in seawater was more accurate, rapid and reliable than either N-ethylcarbazole, or anthrone methods. Artem'yev (1969) examined the phenol method for the determination of the total content of carbohydrates in sediments and came to similar conclusions. Many other authors have adopted this method (e.g. Artem'yev, 1970; Dubois et al. 1956; Faganeli et al. 1987; Gerchakov and Hatcher, 1972; Hitchcock, 1977; Tanoue, 1985) in preference to analysis of individual monosaccharides (e.g. by Brockmann, 1982; Cowie and Hedges, 1984a, b; Hamilton and Hedges, 1988; Handa and Mizuno, 1973; Ittekkot et al. 1984a; Klok et al. 1983; Liebezeit, 1986; Mopper, 1977; Rogers, 1965; Steinberg et al. 1987; Uzaki and Ishiwatari, 1983; Yamaoka, 1983a).

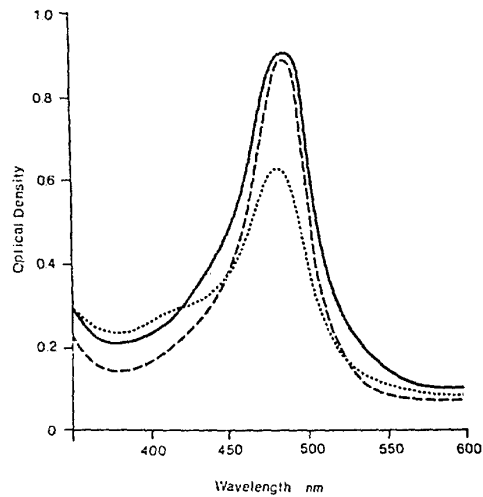


Fig. 3.1. Spectra of agar, starch and lake sediment in phenol-sulphuric acid (Liu et al. 1973).

Key : — agar, --- starch, lake sediment.

The carbohydrate concentrations are measured in terms of mM. The varying responses of different monosaccharides leads to some variance of absorbance (Dubois et al. 1956; Handa, 1966); however, as glucose is a common constituent of polysaccharides and falls in the middle of these variations (Fig.3.2), errors in quantifying carbohydrates by this method should be minimal (Patience et al. 1990).

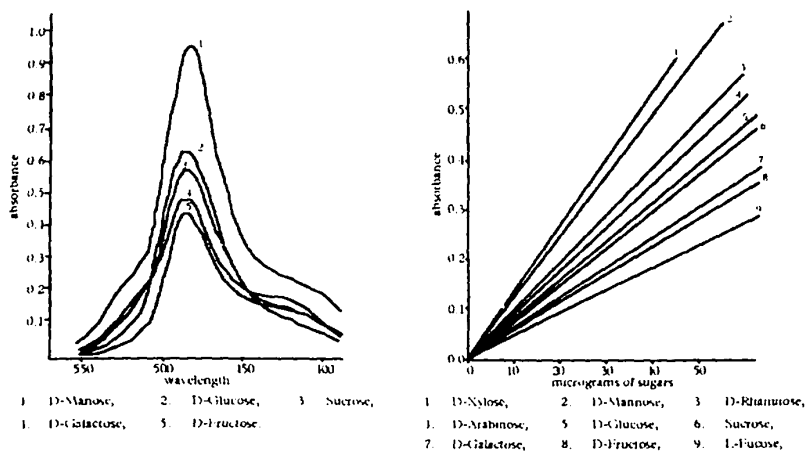


Fig.3.2. Variation in response for different monosaccharides to the phenol-sulphuric acid method (after Handa, 1966).

3.2.2. Cleaning Procedure

All glassware was cleaned by soaking in an acid bath (10% HNO₃, 24 h) and subsequently rinsing in Milli-Q water, and boiling in a solution of Decon-90 (BDH, 2% in Milli-Q water, 24 h). The apparatus was then rinsed in Milli-Q water and dried in an oven (100-140^o C), except for volumetric flasks which were dried at room temperature. The clean glassware was stored in aluminium foil.

3.2.3. Chemicals

The chemicals used for the carbohydrates determinations were as follows:

Milli-Q water for the reagents and standards preparations.

Potassium hydroxide (Fisons Analytical Reagents).

Concentrated Sulphuric acid ('AnalaR' grade, BDH).

Phenol ('AnalaR' grade, BDH).

Glucose ('AnalaR' grade, BDH).

3.2.4. Apparatus

Pyrex culture tubes with screw topped and teflon lined were used for hydrolysis of carbohydrates.

Conical flasks (50 mL).

Volumetric flasks (25 mL).

'Centaur 1' centrifuge (MSE).

3.2.5. Reagent Preparation

Preparation of standard solution

A standard glucose stock solution (~550 μM) for carbohydrate analysis was prepared by dissolution of glucose (25 mg) in water (Milli-Q, 250 mL) and this was used to make a series of standard solutions (~27.5-550 μM) in water (Milli-Q, 25 mL).

Preparation of Phenol solution

Phenol solution (0.53M) was prepared by dissolution of phenol (12.5 g) in water (Milli-Q, 250 mL).

Preparation of Potassium hydroxide solution

Potassium hydroxide solution (0.1M) was prepared by dissolution of potassium hydroxide (1.4 g) in water (Milli-Q, 250 mL).

3.2.6. Extraction of Carbohydrates

The freeze dried and homogenised sediment (~100-200 mg) was weighed in duplicate into clean pre-weighed Pyrex culture tubes (16 x 150 mm), which were sealed with teflon-lined screw caps. A procedural blank of water (Milli-Q, 1 mL) was also included in every batch, H₂SO₄ was then added to the tube (1 mL ; 12 M) and the solution left to stand (2 h) at room temperature. The sample was then diluted (1M) with water (Milli-Q) and hydrolysed (4.5 h ; 100-120⁰ C) in an oven, after which it was allowed to cool. The hydrolysate was centrifuged (3000 r.p.m) and transferred into a conical flask, prior to freezing and freeze-drying (Modulyo Freeze Drier and E2M8 High Vacuum Pump; Edwards). The hydrolysate was redissolved in KOH solution (0.1 mol/L) and made up to 25 mL. The sediment residue left after the first hydrolysis was rehydrolysed as above. The samples were then determined separately for monosaccharide contents.

3.2.7. Determination of Carbohydrates

In the present study, the determination of carbohydrates was carried out after hydrolysis, using the phenol-sulphuric acid method (Patience *et al.* 1990). The details of the analytical method are described below and also shown in Fig. 3.3.

Three aliquots of each standard (2 mL); (27.5 - 550 μ M) were transferred to a series of conical flasks, labelled Ai, Bi and Ci. Phenol solution (2 mL) and sulphuric acid (10 mL) was added to the 'A' series. Water (Milli-Q, 2 mL) and sulphuric acid (10 mL) was added to the 'B' series. Phenol (2 mL) and water (Milli-Q, 10 mL) was added to the 'C' series. All additions were made with rapid mixing. Sediment samples (hydrolysate) were treated identically to the standards.

The solutions were transferred to 1 cm cuvettes, and the absorbances read at 485 nm. Absorbances of the 'A' series were measured *vs.* those of the 'B' series. Phenol absorbance was corrected by measuring the absorbance of the 'C' series *vs.* a blank containing water (Milli-Q, 12 mL) and phenol (2 mL).

A standard curve of corrected absorbance at 485 nm ('A' *vs.* 'B') - 'C' *vs.* glucose standard concentration was constructed (Fig.3.4) and the glucose-equivalent concentrations (mM) in sediment samples were then determined and converted to μ mol g^{-1} dry sediment weight or μ mol (g TOC) $^{-1}$.

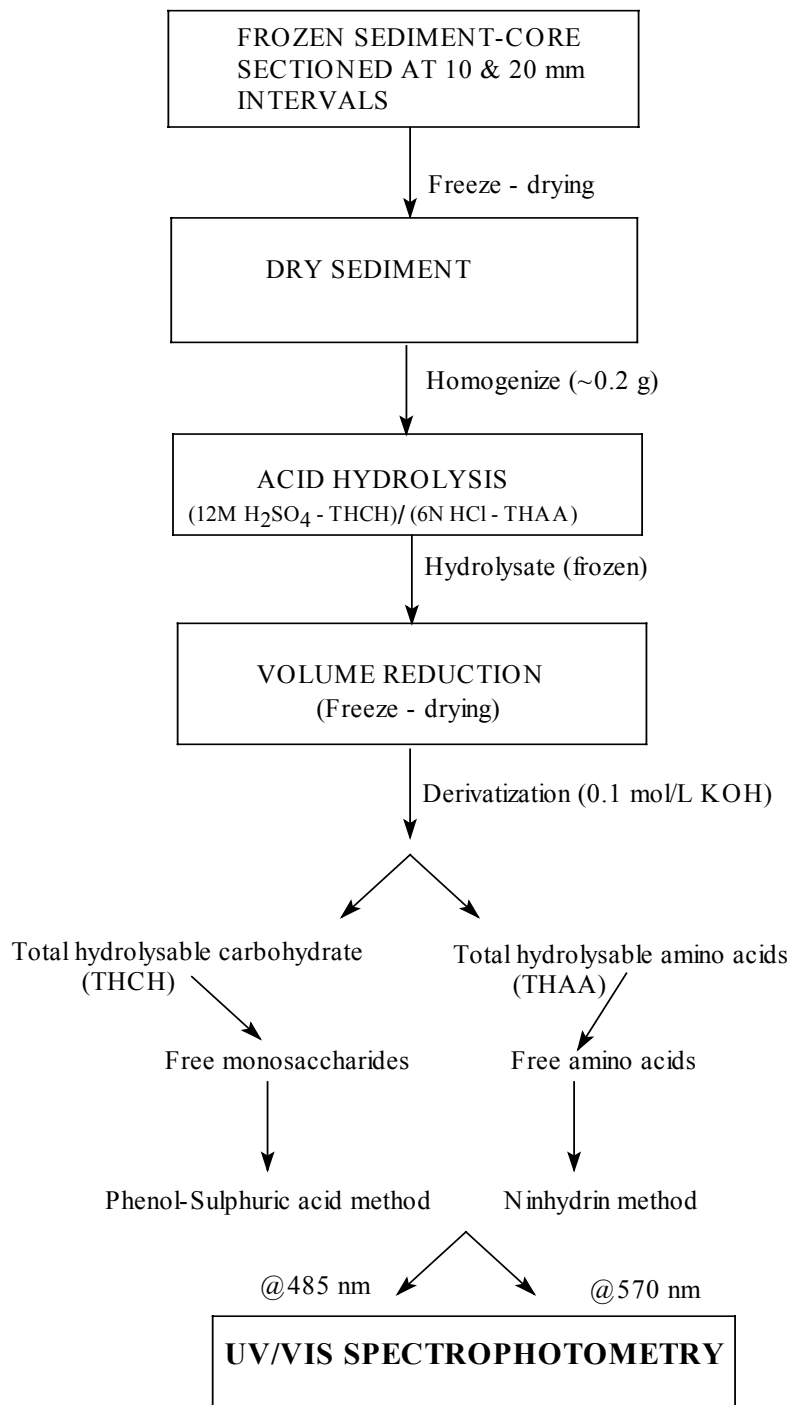


Fig. 3.3. Flow chart of carbohydrate and protein analytical methods

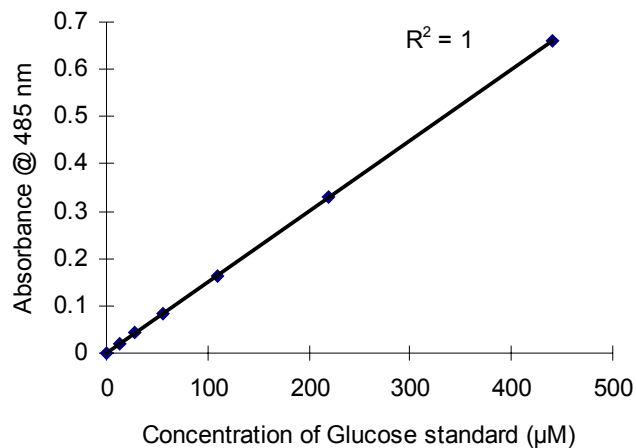


Fig. 3.4. Calibration curve of aqueous Glucose standard.

3.2.8. Reproducibility

In the present study, experiments were carried out to determine the reproducibility of the analytical procedure for carbohydrates using starch as a standard. The efficiency of the hydrolysis procedure was also determined and the results were compared with those for a characterised standard sediment sample (Cargreen mud, Tamar Estuary, UK; supplied by Prof. S. J. Rowland).

3.2.8.1. Preparation of starch solution

Standard starch solution (0.5 mg/mL) was prepared by dissolving starch (50 mg) in hot water (Milli-Q) and dilution to 100 mL. A series of working standards were prepared by diluting aliquots of the stock to obtain the range of concentrations (50-500 mg/mL). A known volume (5 mL; in duplicate) of each solution was pipetted out into clean Pyrex tubes. These solutions were then frozen and freeze-dried.

3.2.8.2. Analysis of starch solution

Hydrolyses were carried out on the dried samples and monosaccharide contents determined. The calibration curve for starch solution (Fig.3.5) showed a similar linear relationship to that of the calibration curve of the glucose standard (Fig.3.4).

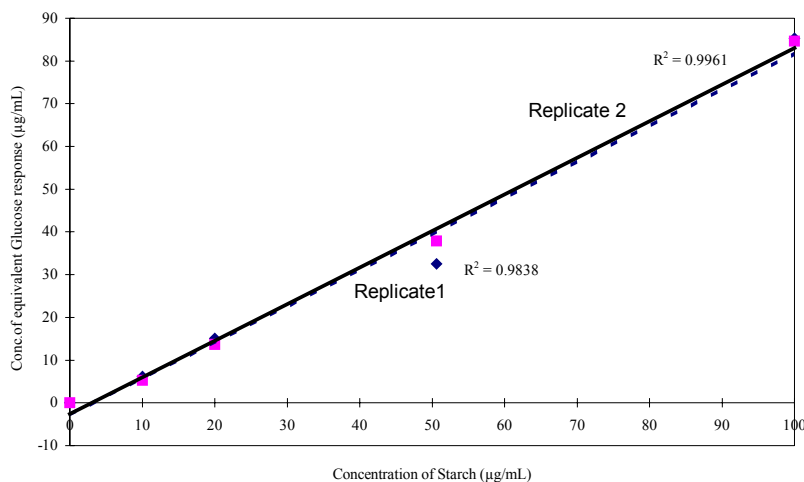


Fig. 3.5. Calibration curve of aqueous starch solution.

3.2.8.3. Analysis of sediment samples

2 gram Cargreen sediment (with conc. 62.9 $\mu\text{mol/g}$) were spiked with 2 mg of starch solution. The replicate analyses ($n = 6$) yielded the carbohydrates concentrations which were reproducible to $\pm 10\%$.

3.2.9. Efficiency of hydrolysis

The efficiency of the hydrolysis procedure for THCH was determined by sequential hydrolysis and analysis of a Arabian Sea abyssal sediment sample. The sediment (~ 0.2 g) was sequentially hydrolysed (x 4); $>90\%$ of THCH was released in the first hydrolysis. No carbohydrates were detected in the third and fourth hydrolysis. Hence in this study, two hydrolyses (in duplicate) were carried out and the sample concentrations combined.

3.3. Protein Analysis

(Total hydrolysable amino acids -THAA)

3.3.1. Introduction

There are a number of methods for the quantification of total proteins (for a review, see Davies, 1988), with the most frequently cited method being that of Lowry et al. (1951). Unfortunately, the Lowry assay suffers from interference by a number of compounds, including free amino acids (Peterson, 1979). Mayer et al. (1986) developed a method for measuring the enzymetically available protein content of sediments. The method was developed to measure total bioavailable protein, available to deposit

feeders. The current techniques for total protein estimation are sensitive to a variety of interfering compounds, which often compromise accurate measurements.

The determination of proteins in recent sediments can be carried out after hydrolysis by characterization of individual amino acids (Degens et al. 1964; Henrichs and Farrington, 1987; Henrichs et al. 1984; Ittekkot et al. 1984a; Klok et al. 1983; Maita et al. 1982; Morris, 1975; Müller et al. 1986; Rosenfeld, 1979; Steinberg et al. 1987; Whelan, 1977) or by quantification using a bulk amino acid assay, such as the ninhydrin method (Rosen, 1957) used here and previously by various authors (Greenfield et al. 1970; Stevenson and Cheng, 1970). The advantage of the latter method is that it is much easier, quicker, and cheaper; the disadvantage is that it quantifies amino groups, not amino acids. The absolute results presented here may thus include a small proportion of compounds that are not amino acids, but which react in the assay, if any such compounds are present.

The ninhydrin test is a colorimetric method involving the formation of a purple colour from the reaction of reduced ninhydrin and amine groups (Rosen, 1957). Amino acids were quantified using a calibration curve set up using known concentrations of glycine. The response variations for different amino acids are negligible, and corrections are not required.

3.3.2. Cleaning Procedure

The apparatus were cleaned in a similar way to that employed for the carbohydrate analysis.

3.3.3. Chemicals

The chemicals used for the determination of proteins are as follows:

Milli-Q water for the reagents and standards preparations.

Stock Sodium Cyanide (0.01 M), (Aldrich, A.C.S Reagent) .

Potassium hydroxide (Fisons Analytical Reagent).

Sodium Acetate (AnalaR grade, BDH).

Acetic acid (glacial, AnalaR grade, BDH).

Ninhydrin (Aldrich, A.C.S Reagent).

2-Methoxy ethanol (Aldrich, Spectrophotometric grade).

2-Propanol (BDH-Hipersolv).

Glycine (AnalaR grade, BDH).

3.3.4. Apparatus

Pyrex culture tubes with teflon-lined screw caps and were used for hydrolyses of proteins.

Conical flasks (50 mL).

Volumetric flasks (25 mL).

Centaur centrifuge.

3.3.5. Reagent Preparation

Preparation of glycine standard solutions

A standard glycine stock solution (10 mM) was prepared by dissolution of glycine (75 mg) in water (Milli-Q, 100 mL) and used to make up a range of concentrations (0.04-0.4 mM).

Preparation of stock Sodium cyanide solution

Sodium cyanide solution (0.01 mol/L) was prepared by dissolution of sodium cyanide (122.5 mg) in water (Milli-Q, 250 mL).

Preparation of Acetate Buffer

Sodium acetate solution (3.96 M) was prepared by dissolving sodium acetate (NaOAc.3H₂O; 54 g) in water (Milli-Q) with addition of glacial acetic acid (10 mL). The final solution was made up to 100 mL.

Preparation of Acetate/Cyanide Buffer

Sodium cyanide in acetate buffer solution (0.2 mM) was prepared by diluting sodium cyanide (1 mL ; 0.01 mol/L) in acetate buffer (50 mL).

Preparation of Ninhydrin solution

Ninhydrin solution (3% wt./vol.) was prepared by dissolving ninhydrin (1.5 g) in methylcellosolve (50 mL).

Preparation of Diluent (2-Propanol/Water, 1:1)

2-Propanol (125 mL) was mixed with water (125 mL) and made up to 250 mL.

Preparation of Potassium hydroxide solution

Potassium hydroxide solution was prepared by dissolving potassium hydroxide (1.4 g) in water (Milli-Q, 250 mL).

3.3.6. Extraction of Proteins

The freeze dried and homogenised sediment (100-200 mg) was weighed, (in duplicate), into clean pre-weighed Pyrex culture tubes with teflon-lined screw caps (16x150 mm). A procedural blank (1 mL, Milli-Q water) was also included with each batch of samples. Then HCl was added (1 mL; 6 M) and hydrolysed in an oven (24 h,

100° C). The samples were removed from the oven and allowed to cool, added water (10 mL, Milli-Q) into the sample, after which the hydrolysates were centrifuged (3000 r.p.m) and transferred into conical flasks prior to freezing and freeze-drying (Modulyo Freeze Drier and E2M8 High Vacuum Pump; Edwards). The hydrolysates were redissolved in KOH solution (0.1 mol/L) and made up to 25 mL. The sediment residues remaining after the first hydrolysis were rehydrolysed as above. The samples were then analysed separately for protein content.

3.3.7. Determination of Proteins

Two aliquots of each standard (1 mL each; 0.04, 0.1, 0.2, 0.3, 0.4 mM), reagent blank and sediment samples (hydrolysate) were transferred into series of Pyrex culture tubes labelled as 'A_i' and 'B_i'. To the 'A' series were added acetate-cyanide (0.5 mL) and ninhydrin solution (0.5 mL). The tubes were immediately capped (loosely) and placed in a sand bath (100°C; 15 min.). After removal from the sand bath, the diluent (2-propanol/water; 10 mL) was added to each of the tubes, which were then shaken and allowed to cool to room temperature. The tubes were then centrifuged for 20 minutes to remove suspended particles that might affect absorbance readings. Aliquots of each solution were then transferred to a 1 cm cuvette, and the absorbance measured at 570 nm *vs.* the reagent blank. A calibration curve of absorbance *vs.* concentration was constructed using the standards. To account for any indigenous colour present in the final reacted unknown solutions, a second set of aliquots (1 mL) of the unknowns were collected in the 'B' series. To these solutions was added water (0.5 mL) and methylcellosolve (0.5 mL); the resulting solutions were heated as before. Recorded absorbances were measured *vs.* a water blank (1.5 mL H₂O, 0.5 mL methylcellosolve

and 10 mL diluent) and the net absorbance subtracted from the value for the reacted solution. The measured absorbance of unknown samples was corrected by subtraction of the blank absorbance values.

A standard curve of corrected absorbance at 570 nm vs. glycine standard concentration was constructed (Fig. 3.6) and the glycine-equivalent concentration (mM) in the samples was then calculated. The concentrations of sediment samples were converted to $\mu\text{mol g}^{-1}$ dry sediment weight.

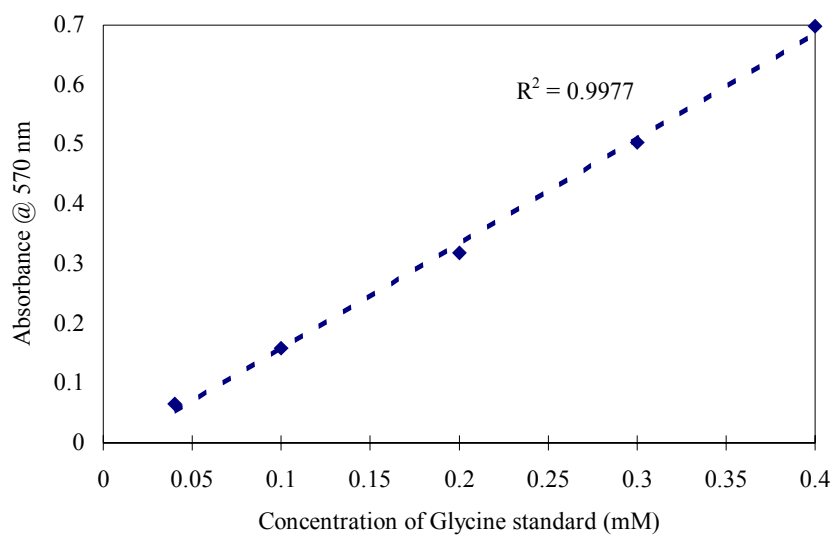


Fig. 3.6. Calibration curve of aqueous glycine standard.

3.3.8. Reproducibility

In order to determine the reproducibility of the analytical procedure a myoglobin-standard was subjected to the hydrolysis and analytical procedures. The efficiency of the hydrolysis was also determined and the results were compared with those for a standard sediment sample (Cargreen mud, Tamar Estuary, UK; supplied by Prof.S.J. Rowland).

3.3.8.1. Preparation of myoglobin solution

Standard myoglobin solution (0.5, 0.1 mg mL⁻¹) was prepared by dissolution of myoglobin (50, 10 mg) in water (Milli-Q,100 mL). A series of working standards were prepared from the stock solutions to obtain the range of concentration (50-500 mg mL⁻¹; 10-100 mg mL⁻¹). A known volume (5 mL; in duplicate) of each solution was pipetted into a clean Pyrex tube. These samples were then frozen and freeze-dried.

3.3.8.2. Analysis of myoglobin solution

Hydrolyses were carried out on the dried samples, and resultant solutions were analysed for protein content as mentioned in section 3.3.7. The calibration curve of myoglobin solution (Fig.3.7) showed a linear relationship similar to that of the glycine standard (Fig.3.6).

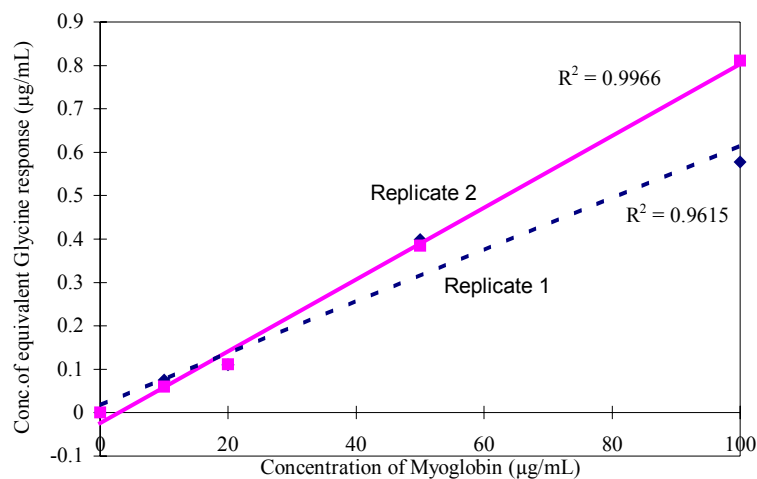


Fig. 3.7. Calibration curve of aqueous myoglobin solution.

3.3.8.3. Analysis of sediment samples

2 gram Cargreen sediment (with conc. 78.5 µmol/g) were spiked with 2 mg of myoglobin solution. The replicate analyses (n = 5) yielded the amino acid concentrations which were reproducible to ±12%.

3.3.9. Efficiency of hydrolysis

The efficiency of the hydrolysis procedure for THAA was determined by sequential hydrolysis and analysis of a Arabian Sea abyssal sediment sample. The sediment (~0.2 g) was sequentially hydrolysed (x 4); >90% of THAA was released in the first hydrolysis. No amino acids were detected in the third and fourth hydrolysis. Hence in this study, two hydrolyses (in duplicate) were carried out and the sample concentrations combined.

3.4. Elemental Analyses

3.4.1. Instrumentation

The elemental compositions of C, H and N of samples in the present study were determined using a Carlo Erba Strumentazine Elemental Analyser model 1106. This instrument performs CHN analyses by combustion of samples in the presence of chromic oxide and copper oxide (1028⁰ C) yielding CO₂, H₂O and a mixture of nitrogen oxides. A secondary reaction tube (containing Cu) removes excess oxygen and reduces nitrogen oxide to nitrogen. The resultant gases are then passed through GC separatory column (2 M Porapak Q 5) and detected by a thermal conductivity detector. Quantitative data were obtained using a Spectra Physics integrator.

3.4.2. Sample Preparations

Total organic carbon (TOC) and total nitrogen (TN) were determined using a modified method of Hedges and Stern (1984). Freeze-dried sediment (~0.15 g, unsieved) was accurately weighed (W_o) in a clean preweighed glass vial. Milli-Q water was added to wet the sample to reduce effervescence during addition of HCl (1M; 2 mL), which was added slowly dropwise and with a gentle rotation of the tube to ensure complete contact of the acid with the sample. The acidified sample was agitated in an ultrasonic bath at room temperature (1/2-1 hrs), centrifuged and the supernatant removed. The acidification was continued until no reaction occurred and again it was agitated and centrifuged. Samples were frozen overnight and then dried in a freeze drier (Modulyo Freeze Drier and E2 MB High Vacuum Pump; Edwards). The sample vials were then reweighed to determine the final sample weight (W_f).

3.4.3. Determination of elemental compositions

Percentage TOC and (%TN) were calculated using the following equation:

$$\%TOC = (100 \times \text{mg OC}) / \text{mg sub sample} \times (W_f / W_o).$$

W_o = Initial weight ; W_f = Final sample weight.

3.4.4. Reproducibility

Replicate analyses (n = 4) of the sample were within the reproducibility $\pm 6\%$.

3.5. Determination of Water Content

The sediment samples collected from the each core-sections were weighed before and after freeze drying to determine their water content.

3.6. Determination of Carbonate Content

Carbonate contents of sediments were determined by weight loss before and after treating the sediment samples with 1 M HCl.

3.7. Clay Minerals

3.7.1. XRD Analyses

Mineralogy was determined by X-ray diffraction only for 3 samples in the different intervals (70-90, 130-150 and 310-330 mm) of the core section (12687#10). The sample powders were scanned from 2 to 60° $2\theta/\text{min}$. on a Siemens X-ray diffractometer (D500 Model), using nickel filtered Cu $K\alpha$ radiation, with DG1 X-ray generator.

3.7.2. Sample Preparations

Briefly, the samples were prepared as follows. The aluminium mounts (square with circle cut from centre) and two glass cover slides were cleaned with tissues. One of the glass slides was fixed to the face of the aluminium mount to be X-rayed with sellotape. Using a small nylon sieve, the hole in the centre of the aluminium mount was carefully filled with sediment samples, to fill the gap so as to be flush with the surface. A new piece of nylon mesh was used for each sample. The other glass slide was then fixed to the top of the mount, prior to its transfer to the diffractometer.

3.8. Micropaleontology (Foraminifera)

The sediments (ca.20 g) were selected from the core section (12687#10) in different intervals (70-90, 130-150 and 310-330 mm) for micropaleontological analyses. The samples were washed in water and collected on a 63 μm sieve. The >63 μm fractions were dried in an oven, but only >250 μm fractions have been studied through the binocular microscope.

3.9. Major elements

3.9.1. Introduction

Sample dissolution is a prerequisite for routine elemental analysis of most types of materials. There are different approach developed for the preparation of geological materials prior to use in ICP analysis, for examples, partial digestions (acid leaches), fusions with alkali fluxes (e.g. Na_2CO_3 , Na_2O_3 , LiBO_2) and acid attacks at both low and high pressures. Some of the methods have been developed for very specific applications (commonly for the determination of only one or a small range of elements) and caution must be exercised when adapting them for multi-element analysis. Alkali fusions are commonly used to digest geological samples for the analysis of major elements by ICP-AES (Thompson and Walsh, 1989). Fusion of rock samples with lithium metaborate results in the formation of glasses which are readily soluble in dilute nitric acid. This procedure is effective for the dissolution of all major rock-forming silicates as well as many accessory minerals (Cremer and Schlocker, 1976; Feldman, 1983). Silica is retained in solution enabling the determination of all major elements from a single preparation. However, the level of total dissolved solids (TDS) in the final solution is limited by instrumental criteria which, to minimize signal drift and maximise precision, require solutions containing <1-2% (ICP-AES) and <0.1-0.2% (ICP-MS) TDS. This requirement restricts the number of trace elements which are quantifiable in fusion preparations. Nevertheless, even with the extra dilution required, fusion has been advocated as the preferred dissolution technique for analysing Ti, Zr, W and Cr (Boumans, 1987), elements which are commonly found in particularly refractory minerals. The dissolution

procedure used in the present study for sample digestion using Lithium metaborate fusion which found to be effective for most refractory minerals.

3.9.2. Sample Analysis

3.9.2.1. Sample Preparations

The decarbonated subsamples (~0.050 g) were mixed carefully with 0.2 g ‘Spectroflux-100B’ (Johnson Matthey®) lithium metaborate and the powders were transferred to a clean (30 mL, pre-ignited®) Ultracarbon graphite crucibles. Samples were fused for 1 hour at 1050° C in a muffle furnace, and the fused beads were cooled. They were then transferred to polypropylene beakers (100-150 mL) containing boiling water (25 mL) and HNO₃ acid (1:1, 1.3 mL). Solutions were stirred continuously with aid of a magnetic stirrer until all solids had dissolved and were then filtered through No.541 filter papers into clean polythene bottles to remove carbon particles, prior to dilution (50 mL).

3.9.2.2. Blank Preparation

The borate blank stock solution was prepared so that it matched 10 times (0.2g x10) the concentration used for the sample decomposition. Borate (10 g) was weighed into a glass beaker. HNO₃ (1:1, 65 mL) was added and the solution was diluted with water (Milli-Q, 250 mL). This was used as a procedural blanks for each batch of samples.

3.9.2.3. Standard Preparation

A series of mixed standards (Spectrosol, BDH) for calcium (1, 5, 10, 20 ppm), magnesium (5, 10, 20, 30 and 40 ppm) and potassium (5, 10, 20 and 40 ppm); a series of standards for titanium (2, 4, 8 and 12 ppm), aluminium (20, 40, 60 and 80 ppm) and silica (6, 12, 18, 24 and 30 ppm) were made up with the addition of appropriate borate blanks, in order to match the matrix effect and finally made up with water (Milli-Q, 50 mL). The sample solutions, blank and standards were stored in clean new polythene bottles were analysed as soon as possible.

3.9.2.4. Instrumentation

Samples were analysed on ICP-AES employing the standard operating conditions used in this laboratory for routine multi-element analysis (Table 3.7). The fusion solutions were analysed for selected major elements (Mg, Ca, K, Si, Ti and Al) using calibrations based on a range of well-characterised standard reference materials (NIM-G, PACS-1; see Govindaraju, 1989 for details). These were chosen to match the range of compositions being studied. Data were interpreted as absolute concentrations and are expressed as weight percent oxides on a carbonate-free basis (CFB) in order to exclude the masking effects of high but variable CaCO_3 contents.

3.9.2.5. Reproducibility

With reference to international standard reference materials (SRM's), the accuracy of measured values of major elements were compared with the established standard reference material values. The absolute accuracy is considered generally to lie within the range of reproducibility (Table 3.8).

3.10. Particle-Size Analysis

3.10.1. Preparation of Calgon

Calgon was prepared by dissolving sodium hexametaphosphate (33 g) and sodium carbonate (7 g) made up with water (Milli-Q, 1000 mL).

3.10.2. Particle-size determinations

The freeze-dried sediment samples collected from each section were weighed (approx. 5 g, if coarse) into the clean glass beaker (100 mL)/conical flask (250 mL). The sample was treated with H₂O₂ (100 vol%, 1 mL) and water (Milli-Q, 1mL) in order to digest organic matter. The samples were heated on a hot plate (~80-90⁰ C) to remove excess H₂O₂. The addition of H₂O₂ and water was continued until the reaction was complete (when fizzing stopped). The final sample was treated with water (Milli-Q, 20 mL) and Calgon (5 mL) to make a suspension which was disaggregated in using ultrasonication (10 minutes) and left overnight. The solution was washed through a

sieve (710 μm size) to remove any coarse materials present. The particle size measurements in each core sections (except 0-10 mm) for both cores were carried out in a Coulter Counter (Model, LS 130). The solutions were injected into the Coulter depending on the volume required to reach the specific obscuration and the results are reported on a volume basis.

Table 3.7. Instrumental Conditions for ICP-AES (Jobin Yvon)

Element	Wavelength (nm)
SiO ₂	251.61
TiO ₂	337.28
Al ₂ O ₃	308.22
MgO	279.55
CaO	422.67
K ₂ O	766.49

Table 3.8. Data obtained for Standard Reference Materials (SRM's) reported as wt% .

Element	PACS-1	Certified value	NIM-G	Certified value
SiO ₂ *	61.44; 63.79; 65.12	55.7	75.35; 73.10; 76.85	75.07
TiO ₂	0.73; 0.74	0.723	0.09; 0.09; 0.10	0.09
Al ₂ O ₃	12.28; 12.41; 12.77	12.23	11.87; 12.16; 12.33	12.08
MgO ₂	2.35; 2.4; 2.4	2.41	0.08; 0.08; 0.08	0.06
CaO	2.98; 3.0; 3.08	2.92	0.74; 0.77; 0.79	0.78
K ₂ O	1.3; 1.38; 1.39	---	4.66; 4.74; 4.88	4.99

*The observed discrepancy for SiO₂ values in PACS-1 may be due to the excessive dilution.

3.11. SAMPLING METHODS

3.11.1. Sampling locations

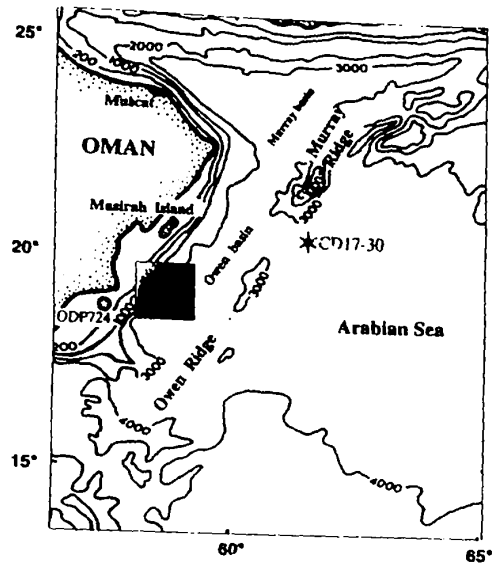
The sampling locations in the Arabian Sea (Oman Margin) are shown in the Figs.3.8(i&ii).

3.11.2. Sample collection

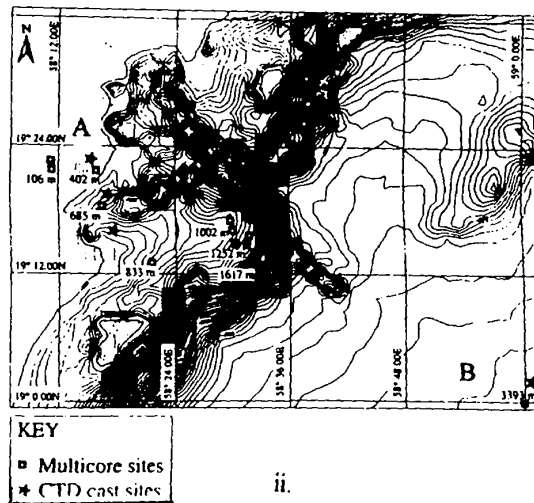
The samples for this study were collected during Cruise 211 on R.R.S. Discovery from 8 th October to 12 th November 1994, from the Arabian Basin at a water depth of approximately 400 m and 3400 m depth. The exact sampling locations of the multi corer (see Figs. 3.8 i&ii) and the core descriptions are presented in Table 3.9.

Table 3.9. Description of Multi-Corer Sampling Stations

Station No	Location	Water depth (m)	Core length (mm)	Date taken
12687 # 8	18° 59'33" N 58° 59.09' E	3372	270-290	20/10/94
12687 # 10	18° 59.42' N 59° 00.92' E	3385	310-330	20/10/94
12690 # 1	19° 22.00' N 58° 15.43' E	377	130-150	22/10/94
12692 # 1	19° 21.83' N 58° 15.42' E	372	130-150	22/10/94
12695# 2	19° 22.07' N 58° 15.43' E	382	130-150	22/10/94



i.



ii.

A & B represent the sites of the samples analysed for the present study.

Figs. 3.8(i&ii). Map showing the sampling locations in the Arabian Sea (Oman Margin).

3.11.3. Sediment core

Sediment cores were collected using a multi-corer (Barnett et al. 1984). Samples were immediately frozen (-20°C) onboard ship prior to transport to the laboratories. They were then freeze-dried in the laboratories. The dried samples were stored (-20° C) prior to analysis. Frozen cores were also collected at this site. Frozen (-20° C) cores were sectioned as follows 0-5 mm, 5-10 mm, 10-70 mm depth with 10 mm intervals, and below 70 mm depth with 20 mm intervals.